Matthew J. Jacobson[1, *], Pascal Flohr[1, 2], Alison Gascoigne[3], Melanie J. Leng[4, 5], Aleksey Sadekov[6], Hai Cheng[7, 8], R. Lawrence Edwards[9], Okan Tüysüz[10], Dominik Fleitmann[1, 11, *]

[1] School of Archaeology, Geography and Environmental Science, University of Reading, Reading, RG6 6UR, UK

[2] Cluster of Excellence ROOTS & Institute for Pre- and Protohistory, University of Kiel, Johanna-Mestorf Straße 2-6, 24118, Kiel, Germany

[3] Archaeology, University of Southampton, Southampton, SO17 1BJ, UK

[4] National Environmental Isotope Facility, British Geological Survey, Keyworth, NG12 5GG, UK

[5] School of Biosciences, University of Nottingham, Loughborough, LE12 5RD, UK

[6] Oceans Graduate School, Faculty of Engineering and Mathematical Sciences, University of Western Australia, Crawley, Perth, Western Australia 6009

[7] Institute of Global Environmental Change, Xi'an Jiatong University, Xi'an 710054, China

[8] Key Laboratory of Karst Dynamics, MLR, Institute of Karst Geology, CAGS, Guilin 541004, China

[9] Department of Earth and Environmental Sciences, University of Minnesota, Minneapolis, MN 55455, USA

[10] Eurasia Institute of Earth Sciences and Department of Geological Engineering, Istanbul Technical University, Istanbul, Turkey

[11] Department of Environmental Sciences, University of Basel, 4056 Basel, Switzerland

*Corresponding authors: Matthew J. Jacobson (m.j.jacobson2@pgr.reading.ac.uk)and Dominik Fleitmann (dominik.fleitmann@unibas.ch)

Key Points:

- Stalagmite Ko-1 record of effective-moisture from SW Turkey stresses spatial and temporal heterogeneity of Turkish climate
- Climate changes share more similarities with other Eastern Mediterranean coastal regions, than central or northern Turkey
- Heterogeneity of modern climate and proxy records highlight the complexity of historical comparisons

Abstract

Palaeoclimate variability must be constrained to predict the nature and impacts of future climate change in the Eastern Mediterranean. Here, we present a high-resolution multiproxy dataset from Kocain Cave, the first of its kind from SW

Turkey. Regional fluctuations in effective-moisture are recorded by variations in magnesium, strontium, phosphorous and carbon isotopes, with oxygen isotopes reacting to changes in precipitation amount and temperature. Important are: a double-peak of arid conditions at 1150 and 800 BCE, a wet period 330-460 CE followed by a rapid shift to dry conditions 460-830 CE, and a distinct dry/wet Medieval Climate Anomaly/Little Ice Age pattern. There are large discrepancies between Turkish records and the Kocain record, which shares more similarities with other Eastern Mediterranean coastal records. Heterogeneity of regional climate and palaeoclimate proxy records are emphasised.

Plain Language Summary

Records of past climate are essential in the Eastern Mediterranean to understand how modern climate change will impact specific regions. By looking at archaeology we can also examine how climate change affected people to prepare for the future. Chemical changes inside stalagmites act as records of past climate; here, we examine one from Kocain Cave, southwest Turkey. Measurements of trace-metals and carbon record the amount of water entering the cave, oxygen records rainfall amount. Ages for the climate changes are calculated using measurements of uranium in the stalagmite. Historical earthquakes that damaged nearby cities and caused tsunamis changed the angle of the stalagmite, providing more evidence for dating the sample.

The Kocain Cave record shows that climate change happened frequently in southwest Turkey. Important are dry conditions 1150 and 800 BCE, wet conditions 330-460 CE followed by a rapid shift to dry conditions 460-830 CE, and a dry/wet Medieval Climate Anomaly/Little Ice Age pattern. These climate changes were different to other records from elsewhere in Turkey and matched better with other coastal records from Greece and Lebanon/Israel. The complex nature of past climate is emphasised due to varied climatic regions in Turkey and the many impacts on each record.

1. Introduction

To predict the nature and impacts of future climate change in the Eastern Mediterranean (E-Med), a "hot-spot" region which will experience severe impacts (Giorgi, 2006), past climatic variability must be constrained (Masson-Delmotte et al., 2013). Paucity of meteorological data (<100 years) renders palaeoclimate records vital for understanding spatial and temporal variance. Likewise, an abundance of archaeological data facilitates analysis of human-climate-environment interactions and resilience of past societies to climatic fluctuations (Luterbacher et al., 2012).

The climate of the E-Med is heterogenous over short distances (Ulbrich et al., 2012). Figure 1 shows highly variable spatial differences in winter precipitation and Old World Drought Atlas (OWDA)-derived Palmer Drought Severity Index (PDSI) for two agricultural drought periods (Cook et al., 2015; University of East Anglia Climatic Research Unit et al., 2020). Agricultural droughts are primarily determined by effective-moisture (EM) and in (semi-)arid regions have a greater

societal impact than individual climatic variables (Dalezios et al., 2017; Jones et al., 2019; Mannocchi et al., 2004). Confidently reconstructing this variability requires a dense network of precisely-dated and highly-resolved palaeoclimate records. Past spatial and temporal climate variability in the E-Med is, however, poorly documented due to unevenly distributed records (Burstyn et al., 2019; Luterbacher et al., 2012).

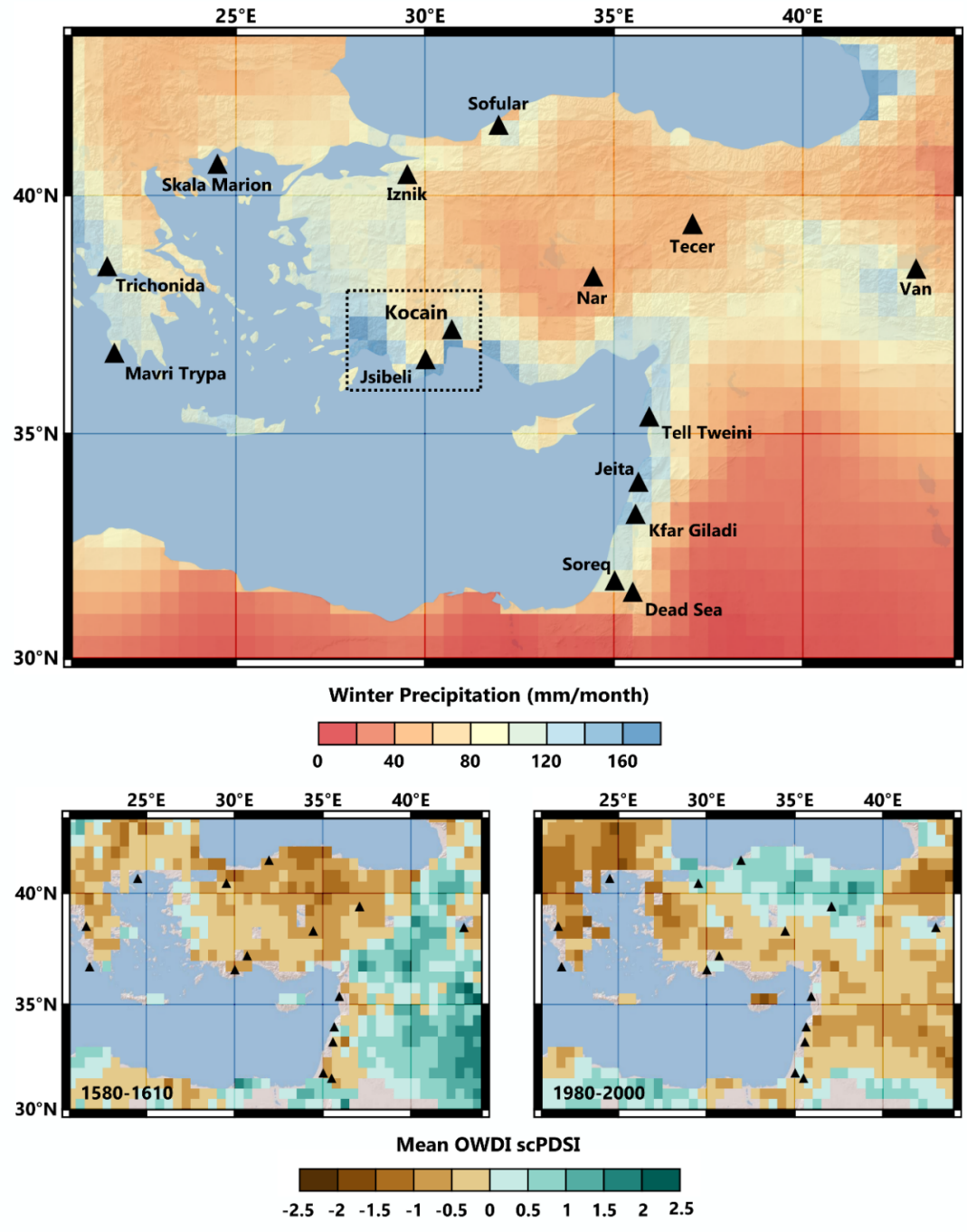

Figure 1: Palaeoclimate archive locations (triangles) compared with CRU

TS4.04 (University of East Anglia Climatic Research Unit et al., 2020) winter (Nov-Mar) precipitation (top) and OWDA-derived PDSI (Cook et al., 2015) during agricultural drought periods (1580-1610 CE and 1980-2000 CE). Dotted square represents SW Turkey (Figure 2c). Data generated in the KNMI Climate Explorer (van Oldenborgh, 2020).

Extensive archaeological and pollen investigations (e.g. Vandam et al., 2019; Woodbridge et al., 2019) make SW Turkey a suitable testbed for examining human-climate-environment interactions. However, high-resolution palaeoclimate datasets from the region only extend back ~1000 (tree-rings) and ~1400 (Lake Salda) years (Danladi and Akçer-Ön, 2018; Heinrich et al., 2013). Stable-isotopes from Lake Gölhisar (Eastwood et al., 2007) reveal low-resolution (~80 years) changes in lake water balance (LWB) throughout the Holocene, albeit with significant dating inaccuracies (±165 years). This record and hydrological tree-rings are seasonally biased towards spring/summer, whereas precipitation mainly occurs in winter (Peterson and Vose, 1997). High-resolution palaeoclimate archives are available from other regions of Turkey (Lake Nar, Sofular Cave); however, these are not local and experience wholly different climatic conditions (Section 5.1).

Here, we fill this gap with a new speleothem record (Ko-1) from Kocain Cave, SW Turkey. We present highly-resolved trace-element (T-E) data starting ~950 BCE, and a stable-isotope record that extends from the present to ~1350 BCE. An age-model is constructed from uranium-series dates (^{230}Th), with supporting evidence from the impact of historically-attested earthquakes on Ko-1. This enables us to establish high-resolution climate variability in SW Turkey for >3000 years during the late Holocene.

2. Cave setting

Kocain Cave (37°13'57" N, 30°42'42" E; 870 m asl), located ~38km north of Antalya, is Turkey's largest cave in terms of opening width (75m) and gallery size (36,000m^2). Kocain has been utilised by humans since the Neolithic and contains a Roman spring-fed cistern, dated by early-Christian inscriptions (Talloen, 2015). Terrain above the cave is covered sparsely by typical Mediterranean vegetation, consisting mainly of evergreen shrubs.

Precipitation (1929-2018; Peterson & Vose, 1997) at Antalya exhibits a marked winter-peak, 90% occurring Nov-Mar, and high inter-annual variability, ranging from 207 mm (2008) to 1914 mm (1969). Alike the entire E-Med (Lionello, 2012; Xoplaki et al., 2018). Moisture is brought by cyclones propelled by westerly storm tracks (Ulbrich et al., 2012) and mountains create sharp contrasts through orographic precipitation caused by rising moist air and associated rain-out effects (Evans et al., 2004). Station data (Figure 2b) reveals that whilst they have similar seasonal patterns, coastal stations (e.g. Antalya) are significantly warmer and wetter than inland stations (e.g. Isparta). Precipitation and temperature are enhanced during negative phases of the North-Sea Caspian Pattern (NCP), Arctic Oscillation (AO), and North Atlantic Oscillation (NAO), likely

linked to increased cyclonic activity and circulation over the warm Mediterranean; however, this pattern is not the same across Turkey (Sariş et al., 2010; Türkeş & Erlat, 2003, 2009; Unal et al., 2012; Section 5.1).

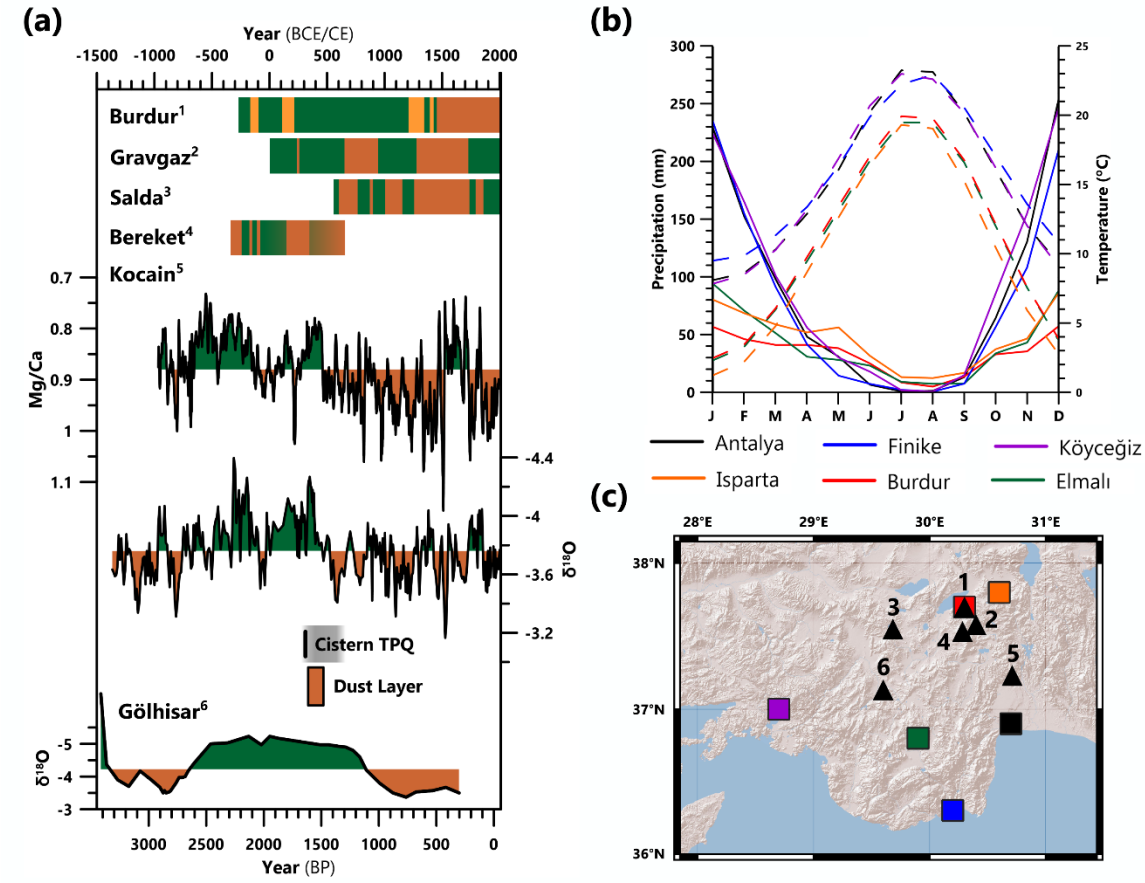

Figure 2: Conditions in the region surrounding Kocain cave. (**a**) Late Holocene palaeohydrological data with periods of high/low EM (green/brown shading), as indicated by original authors (Burdur, Gravgaz, Salda, Bereket) or deviations from the mean (Kocain, Gölhisar). The cistern terminus post quem (312 CE) and Ko-1 dust-layer (335-485 CE) are displayed. (**b**) Average monthly precipitation (solid lines) and temperature (dashed lines) from weather stations in SW Turkey (Peterson & Vose, 1997). (**c**) Map of SW Turkey with proxy records (triangles) and weather stations (squares); colours correspond to stations in 2b.

3. Materials, Methodology and Chronology

The ~350mm, actively-growing stalagmite from Kocain Cave (Ko-1), was collected ~450m from the cave entrance in August 2005. Bedrock thickness above

Ko-1 is ~80 m. A total of 31,503 measurements of T-Es (Ca, Mg, Sr, and P) were performed on the top 156mm at a resolution of ~5µm using Laser Ablation-Inductively Coupled Plasma-Mass Spectrometry (LA-ICP-MS) (Tanner et al., 2002). For oxygen (^{18}O) and carbon (^{13}C) isotope measurements, the first 174.5mm was sampled at intervals of 0.5 mm or less, providing a total of 370 measurements. Further methodological description and sample extraction locations can be found in Text S1 and Figure S2.

For the chronology of Ko-1, 25 ^{230}Th ages were produced (following the analytical protocol of Cheng et al., 2013) ranging from 61±51 to 3387±80 BP (years before 1950 CE). Eight ages affected by significant detrital contamination ($^{230}Th/^{232}Th$ ratios <35) were not included in the age model. The 17 remaining ^{230}Th ages have uncertainties varying from ±38-133 years (M=±67) and only one, at 43mm depth, is not in stratigraphic order. Using these dates and the known collection date (August 2005), a *StalAge* age-model (Scholz and Hoffmann, 2011) was calculated (Figure 3b).

Lateral shifts in the growth-axis at 457±100 CE (87.8 mm) and 176+30/-139 CE (110.3 mm) associated with historically-attested regional earthquakes provide additional evidence for the reliability of the constructed age-model. Tectonic activity altering the cave floor tilt is often a cause for speleothem growth-axis changes (Becker et al., 2006; Cadorin et al., 2001; Forti & Postpischl, 1984; Gilli, 2004; Gilli, 2005). For the ~457 CE displacement, earthquakes in 500, 518 and 528 CE were responsible for destruction of buildings in SW Turkey (Ergin et al., 1967; Gates, 1997; Malalas, 2017; Pirazzoli et al., 1996; Similox-Tohon et al., 2006; Stiros, 2001; Waelkens et al., 2000). The ~176 CE deviation is closely linked to an earthquake in 142 CE which caused extensive damage locally and a tsunami (Altinok et al., 2011; Ambraseys, 2009; Erel and Adatepe, 2007; Kokkinia, 2000; Papadopoulos et al., 2007; Tan et al., 2008). Further details of growth-axis deviations and speleoseismology can be found in Text S2 and Figure S3.

4. Interpretation of the Ko-1 multi-proxy record

^{13}C and ^{18}O from Ko-1 were previously interpreted as reflecting changes in winter temperature and associated snow melt (Göktürk, 2011). New T-E measurements disprove this interpretation, indicating variations in the multi-proxy record can be used to characterise regional fluctuations in EM (Mg/Ca, Sr/Ca), EM/biological activity (P/Ca, ^{13}C), and precipitation amount (^{18}O).

All Ko-1 proxy records correlate and are visually similar as all are linked to EM (Figures 3a and S5). Prior calcite precipitation (PCP) occurs when cave drip-waters reach a gas phase above the cave with lower partial pressure of carbon dioxide (pCO_2) than the soil gas CO_2 with which they were previously in equilibrium (McDonald et al., 2004). This enhances Mg/Ca, Sr/Ca, and ^{13}C ratios, as Ca^{2+} and ^{12}C are preferentially deposited (Fohlmeister et al., 2020; McDermott et al., 2006). Conversely, P accumulates on mineral surfaces during PCP and the P/Ca ratio is thus lowered (Lewis et al., 2011). Additional PCP

occurs in periods of low EM as there are more aerated spaces above the cave and longer aquifer residence times for interaction (Fairchild and Treble, 2009; Treble et al., 2003; Tremaine and Froelich, 2013). A positive correlation between Mg/Ca and Sr/Ca (r=0.57, p<0.0001) provides evidence for PCP (Wassenburg et al., 2020), further supported by strong negative correlations with P/Ca (Mg: r=-0.60, p<0.0001; Sr: r=-0.87, p<0.0001).

Increased EM enhances vegetation cover, soil microbial activity and drip-rates, and causes the ratio between C_3 and C_4 plants to increase (Cheng et al., 2015; Genty et al., 2001). C_4 plants are adapted to warm and (semi-)arid climates and have on average 14‰ less negative ^{13}C than C3 plants (Farquhar, 1983; Farquhar et al., 1989; Henderson et al., 1992). Increased biological activity depletes ^{13}C and releases bio-available P that is transported during periods of intense soil infiltration (Borsato et al., 2007; Fairchild et al., 2001; Johnson et al., 2006; Pote et al., 1999; Treble et al., 2003). A positive correlation between ^{18}O and ^{13}C (r=0.47, p<0.0001) provides evidence for kinetic fractionation, most likely related to fluctuations in the drip-rate (Hendy, 1971). However, the interpretation of ^{18}O in Ko-1 is complicated, as with other Turkish speleothems (see Fleitmann et al., 2009; Göktürk, 2011). Global Network of Isotopes in Precipitation (GNIP) data from Antalya (Figure S6; IAEA/WMO, 2021) show a negative correlation between ^{18}O and precipitation (r=-0.30, p<0.0001; "the amount effect"; Dansgaard, 1964), and a stronger correlation with temperature (r=0.44, p<0.0001). The seasonality of precipitation will alter ^{18}O, with isotopically-lighter ^{18}O precipitated in winter (Nov-Mar; M=–5.6‰, SD=2.1) compared to summer (Jun-Aug; M=–3.4‰, SD=2.6). In Ko-1, more negative ^{18}O coincides with lower Mg/Ca (Figure 3), this relationship can be explained by the importance of precipitation (and temperature) in determining EM (Sinha et al., 2019).

Furthermore, agreement between high magnitude changes in the Ko-1 proxies, and other regional proxies, suggest they reflect EM (Figures 2 and 4; Section 6). Most notable is a distinct phase of high EM (330-460 CE), near-contemporaneous with a distinct brown/orange dust-layer on Ko-1 (335-485 CE; Figure S2) and cistern construction in Kocain Cave (Figure 2). A prominent labarum/*Chi-Rho* symbol ( ) gives this cistern (~250m^3 capacity) a 312 CE *terminus post quem* (earliest possible construction date), as that is when it was incorporated as a shield emblem by Emperor Constantine (Cameron and Hall, 1999), its use remained extensive until the 6th century CE (Hörandner and Carr, 2005). During numerous visits to the cave by the authors between Aug. 2005 and Apr. 2019, this cistern was 0-10% full (0-25m^3) and spring flow was minimal but still occurring. We suggest it was built during a period of greater spring flow and this, combined with the caves large opening width, made it suitable for use by herders. This is further supported by a regional increase in the importance of grazing in the Late Roman Period (300-450 CE), specifically a shift towards goat herding in "marginal" mountainside areas (De Cupere et al., 2017; Fuller et al., 2012; Izdebski, 2012; Poblome, 2015). Animal herds' use of the cistern would have kicked-up fine dust from the cave floor, which was then

incorporated into the stalagmite. This mechanism could explain the dust-layer; which would usually suggest drier conditions if corresponding to increases in Mg/Ca (see Carolin et al., 2019).

Local palaeoenvironmental evidence suggests high EM in the 4^{th} and early 5^{th} centuries CE as indicated by wild weeds that require high soil quality and moisture availability growing in the territory of Sagalassos (Bakker et al., 2012; Kaniewski et al., 2007); wetland conditions and spring reactivation in the Bereket Valley and Gravgaz Marsh (Bakker et al., 2013; Kaptijn et al., 2013; Van Geel et al., 1989; Vermoere et al., 2002); and deep-water conditions at Lake Burdur (Tudryn et al., 2013). Similar changes are evidenced in E-Med proxies, suggesting this wet phase was a regional phenomenon (see below). The above interpretations, and corroborating evidence, strengthen our claim that decreases in Ko-1 Mg/Ca, Sr/Ca, ^{13}C and ^{18}O, with increases in P/Ca, are indicative of wetter climatic conditions in SW Turkey.

5. Eastern Mediterranean Palaeoclimate

Palaeohydrological changes for SW Turkey are reflected in geochemical proxies (Mg/Ca, Sr/Ca, P/Ca, ^{18}O, ^{13}C) in Ko-1 (Figures 3, S4 and S5). First, distinct phases of low EM are centred at ~1150 and ~800 BCE, with an intervening wet phase between ~1000 and 900 BCE. Secondly, high EM occurred between ~330 and 460 CE, followed by a rapid shift to drier conditions that lasted until ~830 CE. Finally, during the Medieval Climate Anomaly (MCA; 850-1300 CE) and Little Ice Age (LIA; 1400-1700 CE), there was enhanced variability in EM, especially during 1450-1550 CE, and a dry/wet MCA/LIA pattern.

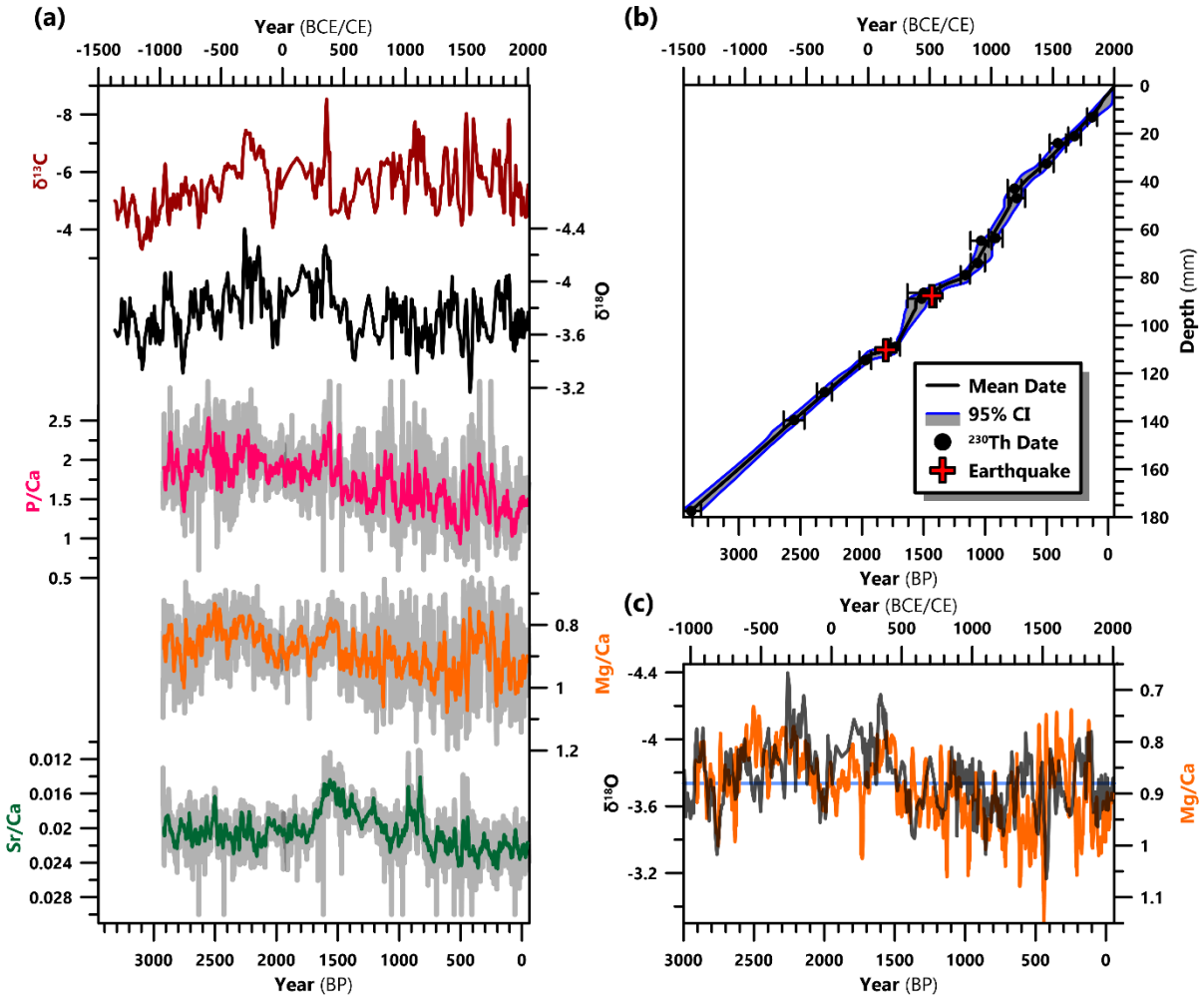

Figure 3: Stable-isotope (‰) and trace-element (mmol/mol^{-1}) palaeoclimate proxy records from Kocain Cave. (**a**) Ko-1 proxies aligned so peaks represent wetter conditions. Trace-elements are displayed as annual (grey) and 15-year (colours) averages. (**b**) *StalAge* model for Ko-1. Earthquakes were not input to the model. (**c**) Comparison between Mg/Ca and ^{18}O. Blue line represents the mean value of both records (0.88mmol/mol^{-1} and –3.8‰).

Marked palaeohydrological changes between 1200 and 750 BCE are widespread (e.g. Park et al., 2019) and often associated with cold phases, such as the so-called 3.2 and 2.8 ka events and Crisis Years Cooling Event (CYCE), and reductions in solar irradiance (Kaniewski et al., 2019; Mayewski et al., 2004; Steinhilber et al., 2009; Wanner et al., 2015). Links between these changes and socio-political change remain controversial (Drake, 2012; Finné et al., 2017; Kaniewski et al., 2013; Knapp and Manning, 2016; Manning et al., 2020). While

similar palaeohydrological changes to those revealed by Ko-1 are observed in records such as Gölhisar, Skala Marion, and Tell Tweini (Eastwood et al., 2007; Kaniewski et al., 2019; Psomiadis et al., 2018), others are dissimilar (Figure 4). No aridification is observed at Sofular, Nar, or Tecer (Dean et al., 2018; Fleitmann et al., 2009; Göktürk et al., 2011; Jones et al., 2006; Kuzucuoğlu et al., 2011), whereas a single shift to more arid conditions is evidenced at Iznik, Van, Mavri Trypa, Jeita, Soreq, and in the Middle East in general (Bar-Matthews et al., 2003; Barlas Şimşek and Çağatay, 2018; Cheng et al., 2015; Finné et al., 2017; Sinha et al., 2019; Ülgen et al., 2012).

Wet conditions between ~330 and 460 CE rapidly shift to an arid phase between ~460 and 830 CE in the Ko-1 record, roughly coincident with the Dark Ages Cold Period (DACP: 450-800 CE; Helama et al., 2017; Figure 4). An EM peak in SW Turkey is supported by local archaeological and palaeoenvironmental evidence, as well as features of Kocain cave (see above). Similar wet peaks are observed across the E-Med at ~300-500 CE. Speleothem ^{18}O from Mavri Trypa and Skala Marion caves demonstrate wet conditions at ~300-350 CE (Finné et al., 2017; Psomiadis et al., 2018). EM proxies from Lake Trichonida show an apparently delayed response, with the records wettest phase between ~420 and 500 CE (Seguin et al., 2020). Reconstructed precipitation based on Dead Sea data suggests ~350-490 CE may be the wettest interval in the late Holocene for the southern Levant, whereas a depletion of isotopes from Jeita Cave suggests a break from arid conditions between ~320 and 400 CE (Bookman et al., 2004; Cheng et al., 2015; Morin et al., 2019).

Generally, these wet phases are followed by a rapid shift to drier conditions in the 5^{th} century (Figure 4). This pre-dates the Late Antique Little Ice Age (LALIA)/"536-550 CE climate downturn" (Büntgen et al., 2016; Newfield, 2018), a phasing that is also observed in records from the Middle East (e.g. Sharifi et al., 2015). However, other Turkish records show very different palaeohydrological changes. Locally, wet conditions prevailed longer: high detrital and low carbonate content at the start of the Lake Salda record (~550-600 CE) indicate wet conditions, cluster analysis of pollen and non-pollen palynomorphs from Gravgaz Marsh reveal wet conditions until 640 CE, and ^{18}O from Gölhisar remains depleted until ~800 CE (Bakker et al., 2011; Danladi & Akçer-Ön, 2018; Eastwood et al., 2007). Records from northern (Sofular), central (Nar, Tecer) and eastern (Van) Turkey show the inverse to Ko-1, with a marked dry phase starting ~300-350 CE, followed by a shift to humid conditions ~500-550 CE that endured for centuries (Barlas Şimşek and Çağatay, 2018; Dean et al., 2018; Fleitmann et al., 2009; Kuzucuoğlu et al., 2011).

Enhanced variation in EM is evidenced in the Ko-1 record from ~800 until 1850 CE (Figures 3 and 4). From ~900 CE until ~1460 CE, dry conditions prevailed, with more-humid intervals every ~120-150 years (~1030, ~1180, ~1300 CE), encompassing the MCA (850-1300 CE). Hydroclimate was especially turbulent between ~1450 and 1550 CE, experiencing an extreme dry-wet-dry-wet pattern. The driest conditions in the entire Ko-1 record occur between 1510-1530 CE,

indicated by the highest ^{18}O value and 15-year Mg/Ca average. Subsequently, EM was still highly variable but consistently elevated until ~1750 CE, a period roughly coincident with the LIA (1400-1850 CE). Reconstructed winter-spring temperatures from Jsibeli in SW Turkey suggest cooling after ~1500 CE, with the coldest conditions at ~1750 CE (Heinrich et al., 2013), when there was a break from high EM at Kocain (Figure 4). Higher EM is evidenced again in the Ko-1 Mg/Ca and ^{18}O records during from 1810 to 1840 CE, coincident with a short return to colder conditions at Jsibeli (Heinrich et al., 2013) resulting from the Dalton solar minimum and the 1815 Tambora eruption (Cole-Dai et al., 2009).

The dry/wet MCA/LIA pattern observed at Kocain contrasts with other records from Turkey (Burdur, Salda, Nar, Sofular, Iznik), which appear to show the inverse pattern (Danladi and Akçer-Ön, 2018; Dean et al., 2015; Fleitmann et al., 2009; Tudryn et al., 2013; Ülgen et al., 2012), and from the Fertile Crescent (Jeita, Kfar Giladi, Soreq, Gejkar, Neor), which show no pattern (Bar-Matthews et al., 2003; Cheng et al., 2015; Flohr et al., 2017; Luterbacher et al., 2012; Morin et al., 2019; Sharifi et al., 2015; Figures 4 and S7). Most high-resolution Greek/Aegean records do not cover this more recent time interval. However, Trichonida log(Rb/Sr) exhibits strong similarities to Ko-1 (Figure 4). Dry conditions ~900-1450 CE follow a wetter phase ~850 CE, with breaks at 1050 and 1300 CE. Increased EM is then demonstrated until 1650 CE, before another peak in the early 19^{th} century CE, also evidenced in Nar diatom ^{18}O (Dean et al., 2018; Seguin et al., 2020).

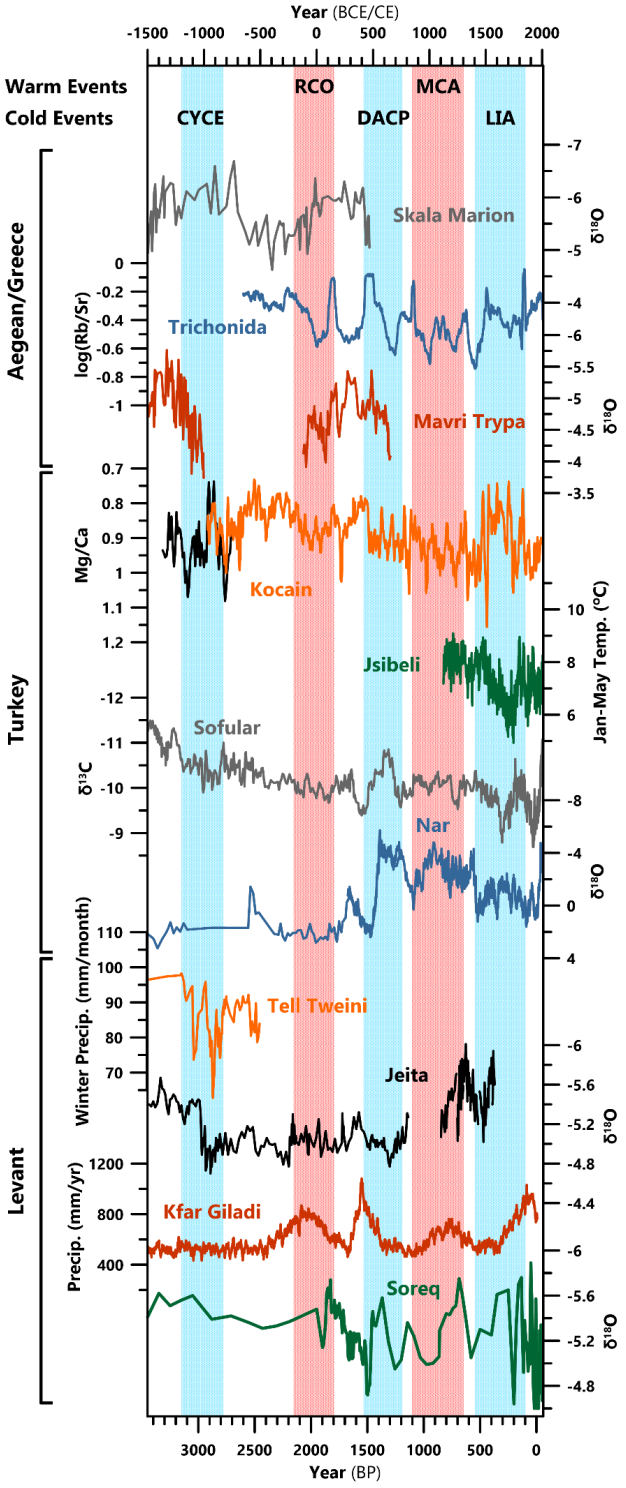
Year (BCE/CE)
-1500 -1000 -500 0 500 1000 1500 2000
Warm Events
Cold Events
RCO
MCA
CYCE
DACP
LIA
Aegean/Greece
Turkey
Levant
Skala Marion
Trichonida
Mavri Trypa
Kocain
Jsibeli
Sofular
Nar
Tell Tweini
Jeita
Kfar Giladi
Soreq
log(Rb/Sr)
Mg/Ca
δ13C
Winter Precip. (mm/month)
Precip. (mm/yr)
δ18O
Jan-May Temp. (°C)
3000 2500 2000 1500 1000 500 0
Year (BP)

Figure 4: Eastern Mediterranean palaeoclimate proxies compared with Ko-1 Mg/Ca (15-year averages) and ^{18}O (black; prior to 750 BCE), peaks represent wetter conditions (excl. Jsibeli). Warm/cold events (red/blue shaded areas, respectively) are: Crisis Years Cold Event (CYCE), Roman Climatic Optimum (RCO), Dark Ages Cold Period (DACP), Medieval Climate Anomaly (MCA), and Little Ice Age (LIA). For references, see text.

5.1. Heterogeneity of Eastern Mediterranean climate and proxies

Overall, there are large discrepancies between the Ko-1 record of EM and other hydrological proxies from the wider E-Med. There are three main causes for these discrepancies, which will be discussed further below: (1) spatial climate variations and challenges in palaeoclimate analysis, related to (2) interpretation of different types of proxies with varied sensitivity to hydroclimatic change and (3) chronological uncertainties. The greatest differences between records discussed here are observed between Ko-1 and other records from Turkey. Climatic heterogeneity in SW Turkey is more extreme across the country, which is large (780,000km^2), has complex and diverse topography, and numerous moisture sources (Lionello, 2012; Xoplaki et al., 2018). These factors lead regions to have varied temperatures (Aydın et al., 2019), seasonal patterns (Sariş et al., 2010), and impacts from teleconnections (Unal et al., 2012).

The two other high-resolution Turkish records that contrast with Ko-1, Lake Nar (central Anatolian plateau: CAP) and Sofular Cave (NW Turkey; Black Sea coast), are in different climatic regions. The high elevation CAP region experiences low precipitation, with two peaks (Apr.-May/Oct.-Dec.), and cold semi-arid and dry continental climates (Öztürk et al., 2017; Peel et al., 2007). The Black Sea coast is temperate, with precipitation of a similar magnitude to SW Turkey, but there is no dry season and precipitation is high throughout the year (Göktürk et al., 2011; Karaca et al., 2000). The impact of large-scale atmospheric teleconnections (NCP, AO, NAO) also differs in these regions, compared to SW Turkey which has enhanced precipitation and temperature during negative phases (Kutiel et al., 2002; Sezen and Partal, 2019). Negative phases cause higher temperatures across Turkey, particularly in winter. However, the CAP experiences significantly greater increases (Kutiel and Türkeş, 2005; Türkeş and Erlat, 2009). Impacts on precipitation are more varied. The Black Sea weakens the impacts of teleconnections on precipitation in NW Turkey (Göktürk et al., 2011; Türkeş and Erlat, 2003). AO- and NCP- phases cause their most significant impact on precipitation in SW Turkey (Kutiel and Benaroch, 2002), with CAP only impacted by AO- phases in winter (Sezen and Partal, 2019) and the transition between enhancements/reductions in precipitation from NCP- phases located <50km from Nar (Kutiel et al., 2002; Kutiel and Türkeş, 2005). NAO influence is weaker and focused on the western and central regions (Unal et al., 2012). These differences lead to spatial variations in droughts (Figures 1 and S8; Vicente-Serrano et al., 2010). Turkish records respond differently because of this variability. Lake Nar records LWB, with higher ^{18}O corresponding to hydrological droughts (lake-water deficits) (Jones et al., 2019). Speleothems

record fluctuations in EM, which are more akin to agricultural droughts (soil-moisture availability) (Fleitmann et al., 2009; Göktürk et al., 2011). However, none of these records are simple, being influenced by multiple climatic and regional factors, the importance of which may change over time. Additionally, proxies represent different seasons. ^{18}O is taken from carbonates at Lake Nar, primarily deposited in early summer in response to evaporation and aridity (Dean et al., 2015). Speleothem records are winter-season biased due to seasonality of precipitation (Kocain only) and the lighter-isotope signature of winter precipitation.

The impact of temperature change on precipitation and proxy records is also poorly understood and varied. Antalya GNIP data shows a negative correlation between precipitation and temperature ($r=-0.53$, $p<0.0001$; Figure S6) and lower temperatures during the CYCE correspond to precipitation reductions. However, cooler temperatures during the LIA correspond to increased EM at Kocain Cave (Figure 4).

Comparison between records is further complicated by chronological uncertainties of decadal-centurial length in lake and speleothem records. Multiple and varied lags are present between climatic changes in different regions, and between climatic shifts and their signal in records. Different resolutions hinder comparison and the specifics of resolutions, i.e., whether a sample is an average across a large period or a specific point in time, are rarely addressed.

6. Conclusion

Stalagmite Ko-1 provides the first highly-resolved, well-dated palaeohydrological proxy record covering the late Holocene for SW Turkey. Key periods of palaeoclimatic change are revealed, notably: (1) a double-peak of arid conditions (1150 and 800 BCE), (2) a distinct period of high EM in the 4^{th} and 5^{th} centuries CE (~330 to 460 CE), followed by (3) a rapid shift to low EM (460 CE) that persisted until ~830 CE, and finally (4) a distinct dry/wet MCA/LIA pattern. Changes were often in contrast to palaeoclimate records from northern and central Turkey, and sometimes locally, more frequently correlating with changes in coastal records from the Aegean and Levant. Considering the heterogeneity of climate and the multitude of impacts on records, palaeoclimatic interpretations are complex and care must be taken especially when they are utilised for discussions of societal impacts.

Acknowledgments, Samples, and Data

The new Kocain speleothem uranium-series, trace-element and stable-isotope data used in this study are available in the NOAA palaeoclimate archive via LINK – archiving is underway but not finalised. This work was supported by the AHRC South, West and Wales Doctoral Training Partnership (Grant AH/L503939/1 to MJJ), the Swiss National Science Foundation (Grant PP002-110554/1 to DF), the U.S. National Science Foundation (Grant 1702816 to RLE), the ERC Advanced Grant (2010 NEWLOG ADG-267931 to AS, awarded to Prof. H. Elderfield) and the National Natural Science Foundation of China (Grant

NSFC 41888101 to HC). The isotope and trace-element data were provided by the National Environmental Isotope Facility and the Department of Earth Science, University of Cambridge, respectively.

References

Altinok, Y., Alpar, B., Özer, N., Aykurt, H., 2011. Revision of the tsunami catalogue affecting Turkish coasts and surrounding regions. Nat. Hazards Earth Syst. Sci. 11, 273–291. https://doi.org/10.5194/nhess-11-273-2011Ambraseys, N., 2009. Earthquakes in the eastern Mediterranean and the Middle East: a multidisciplinary study of 2000 years of seismicity. Cambridge University Press, Cambridge.Aydın, S., Şimşek, M., Çetinkaya, G., Öztürk, M.Z., 2019. Erinç Yağış Etkinlik İndisi'ne Göre Belirlenen Türkiye İklim Bölgelerinin Rejim Karakteristikleri (Regime Characteristiscs of Turkey's Climatic Regions Determined Using the Erinç Precipitation Efficiency Index), in: 1st Istanbul International Geography Congress Proceedings Books. Istanbul University Press, Istanbul, pp. 752–760. https://doi.org/10.26650/PB/PS12.2019.002.074Bakker, J., Kaniewski, D., Verstraeten, G., De Laet, V., Waelkens, M., 2011. the southwest Taurus Mountains, Turkey Numerically derived evidence for late-Holocene climate change and its impact on human presence in. https://doi.org/10.1177/0959683611425546Bakker, J., Paulissen, E., Kaniewski, D., de Laet, V., Verstraeten, G., Waelkens, M., 2012. Man, vegetation and climate during the Holocene in the territory of Sagalassos, Western Taurus Mountains, SW Turkey. Veg. Hist. Archaeobot. 21, 249–266. https://doi.org/10.1007/s00334-011-0312-4Bakker, J., Paulissen, E., Kaniewski, D., Poblome, J., De Laet, V., Verstraeten, G., Waelkens, M., 2013. Climate, people, fire and vegetation: New insights into vegetation dynamics in the Eastern Mediterranean since the 1st century AD. Clim. Past 9, 57–87. https://doi.org/10.5194/cp-9-57-2013Bar-Matthews, M., Ayalon, A., Gilmour, M., Matthews, A., Hawkesworth, C.J., 2003. Sea–land oxygen isotopic relationships from planktonic foraminifera and speleothems in the Eastern Mediterranean region and their implication for paleorainfall during interglacial intervals. Geochim. Cosmochim. Acta 67, 3181–3199.Barlas Şimşek, F., Çağatay, M.N., 2018. Late Holocene high resolution multi-proxy climate and environmental records from Lake Van, eastern Turkey. Quat. Int. 486, 57–72. https://doi.org/10.1016/j.quaint.2017.12.043Becker, A., Davenport, C.A., Eichenberger, U., Gilli, E., Jeannin, P.Y., Lacave, C., 2006. Speleoseismology: A critical perspective. J. Seismol. 10, 371–388. https://doi.org/10.1007/s10950-006-9017-zBookman, R., Enzel, Y., Agnon, A., Stein, M., 2004. Late Holocene lake levels of the dead sea. Bull. Geol. Soc. Am. 116, 555–571. https://doi.org/10.1130/B25286.1Borsato, A., Frisia, S., Fairchild, I.J., Somogyi, A., Susini, J., 2007. Trace element distribution in annual stalagmite laminae mapped by micrometer-resolution X-ray fluorescence: Implications for incorporation of environmentally significant species. Geochim. Cosmochim. Acta 71, 1494–1512. https://doi.org/10.1016/j.gca.2006.12.016Büntgen, U., Myglan, V.S., Ljungqvist, F.C., McCormick, M., Di Cosmo, N., Sigl, M., Jungclaus, J., Wagner, S., Krusic, P.J., Esper, J., Kaplan, J.O., De Vaan, M.A.C.,

Luterbacher, J., Wacker, L., Tegel, W., Kirdyanov, A. V., 2016. Cooling and societal change during the Late Antique Little Ice Age from 536 to around 660 AD. Nat. Geosci. 9, 231–236. https://doi.org/10.1038/ngeo2652Burstyn, Y., Martrat, B., Lopez, Jordi, F., Iriarte, E., Jacobson, M.J., Lone, M.A., Deininger, M., 2019. Speleothems from the Middle East: An Example of Water Limited Environments in the SISAL Database. Quaternary 2. https://doi.org/10.3390/quat2020016Cadorin, J.F., Jongmans, D., Plumier, A., Camelbeeck, T., Delaby, S., Quinif, Y., 2001. Modelling of speleothems failure in the Hotton cave (Belgium). Is the failure earthquake induced? Netherlands J. Geosci. 80, 315–321. https://doi.org/10.1017/S001677460002391XCameron, A., Hall, S., 1999. Eusebius of Caesarea: Vita Constantini (Life of Constantine). Oxford University Press, New York.Carolin, S.A., Walker, R.T., Day, C.C., Ersek, V., Alastair Sloan, R., Dee, M.W., Talebian, M., Henderson, G.M., 2019. Precise timing of abrupt increase in dust activity in the Middle East coincident with 4.2 ka social change. Proc. Natl. Acad. Sci. U. S. A. 116, 67–72. https://doi.org/10.1073/pnas.1808103115Cheng, H., Lawrence Edwards, R., Shen, C.C., Polyak, V.J., Asmerom, Y., Woodhead, J., Hellstrom, J., Wang, Y., Kong, X., Spötl, C., Wang, X., Calvin Alexander, E., 2013. Improvements in 230 Th dating, 230 Th and 234 U half-life values, and U-Th isotopic measurements by multi-collector inductively coupled plasma mass spectrometry. Earth Planet. Sci. Lett. 371–372, 82–91. https://doi.org/10.1016/j.epsl.2013.04.006Cheng, H., Sinha, A., Verheyden, S., Nader, F.H., Li, X.L., Zhang, P.Z., Yin, J.J., Yi, L., Peng, Y.B., Rao, Z.G., Ning, Y.F., Edwards, R.L., 2015. The climate variability in northern Levant over the past 20,000 years. Geophys. Res. Lett. 42, 8641–8650. https://doi.org/10.1002/2015GL065397Cole-Dai, J., Ferris, D., Lanciki, A., Savarino, J., Baroni, M., Thiemens, M.H., 2009. Cold decade (AD 1810–1819) caused by Tambora (1815) and another (1809) stratospheric volcanic eruption. Geophys. Res. Lett. 36, L22703. https://doi.org/10.1029/2009GL040882Cook, E.R., Seager, R., Kushnir, Y., Briffa, K.R., Büntgen, U., Frank, D., Krusic, P.J., Tegel, W., van der Schrier, G., Andreu-Hayles, L., Baillie, M., Baittinger, C., Bleicher, N., Bonde, N., Brown, D., Carrer, M., Cooper, R., Čufar, K., Dittmar, C., Esper, J., Griggs, C., Gunnarson, B., Günther, B., Gutierrez, E., Haneca, K., Helama, S., Herzig, F., Heussner, K.-U., Hofmann, J., Janda, P., Kontic, R., Köse, N., Kyncl, T., Levanič, T., Linderholm, H., Manning, S., Melvin, T.M., Miles, D., Neuwirth, B., Nicolussi, K., Nola, P., Panayotov, M., Popa, I., Rothe, A., Seftigen, K., Seim, A., Svarva, H., Svoboda, M., Thun, T., Timonen, M., Touchan, R., Trotsiuk, V., Trouet, V., Walder, F., Ważny, T., Wilson, R., Zang, C., 2015. Old World megadroughts and pluvials during the Common Era. Sci. Adv. 1, e1500561. https://doi.org/10.1126/sciadv.1500561Dalezios, N.R., Gobin, A., Tarquis Alfonso, A.M., Eslamian, S., 2017. Agricultural Drought Indices: Combining Crop, Climate, and Soil Factors, in: Eslamian, S., Eslamian, F. (Eds.), Handbook of Drought and Water Scarcity: Environmental Impacts and Analysis of Drought and Water Scarcity. CRC Press, Boca Raton, pp. 73–89. https://doi.org/10.1201/9781315404219-5Danladi, I.B., Akçer-Ön, S., 2018. Solar forcing and climate variability during the past millennium as recorded

in a high altitude lake: Lake Salda (SW Anatolia). Quat. Int. 486, 185–198. https://doi.org/10.1016/j.quaint.2017.08.068Dansgaard, W., 1964. Stable isotopes in precipitation. Tellus 16, 436–468. https://doi.org/10.3402/tellusa.v16i4.8993De Cupere, B., Frémondeau, D., Kaptijn, E., Marinova, E., Poblome, J., Vandam, R., Van Neer, W., 2017. Subsistence economy and land use strategies in the Burdur province (SW Anatolia) from prehistory to the Byzantine period. Quat. Int. 436, 4–17. https://doi.org/10.1016/j.quaint.2015.11.097Dean, J.R., Jones, M.D., Leng, M.J., Metcalfe, S.E., Sloane, H.J., Eastwood, W.J., Roberts, C.N., 2018. Seasonality of Holocene hydroclimate in the Eastern Mediterranean reconstructed using the oxygen isotope composition of carbonates and diatoms from Lake Nar, central Turkey. Holocene 28, 267–276. https://doi.org/10.1177/0959683617721326Dean, J.R., Jones, M.D., Leng, M.J., Noble, S.R., Metcalfe, S.E., Sloane, H.J., Sahy, D., Eastwood, W.J., Roberts, C.N., 2015. Eastern Mediterranean hydroclimate over the late glacial and Holocene, reconstructed from the sediments of Nar lake, central Turkey, using stable isotopes and carbonate mineralogy. Quat. Sci. Rev. 124, 162–174. https://doi.org/10.1016/j.quascirev.2015.07.023Drake, B.L., 2012. The influence of climatic change on the Late Bronze Age Collapse and the Greek Dark Ages. J. Archaeol. Sci. 39, 1862–1870. https://doi.org/10.1016/j.jas.2012.01.029Eastwood, W.J., Leng, M.J., Roberts, N., Davis, B., 2007. Holocene climate change in the eastern Mediterranean region: A comparison of stable isotope and pollen data from Lake Gölhisar, southwest Turkey. J. Quat. Sci. 22, 327–341. https://doi.org/10.1002/jqs.1062Erel, T., Adatepe, F., 2007. Traces of historical earthquakes in the ancient city life at the Mediterranean region. J. Black Sea / Mediterr. Environ. 13, 241–252.Ergin, K., Guclu, U., Uz, Z., 1967. A Catalog of Earthquakes for Turkey and the Surrounding Area (11 A.D. to 1964 A.D.). Istanbul Technical Univeristy, Istanbul.Evans, J.P., Smith, R.B., Oglesby, R.J., 2004. Middle East climate simulation and dominant precipitation processes. Int. J. Climatol. 24, 1671–1694. https://doi.org/10.1002/joc.1084Fairchild, I.J., Baker, A., Borsato, A., Frisia, S., Hinton, R.W., McDermott, F., Tooth, A.F., 2001. Annual to sub-annual resolution of multiple trace-element trends in speleothems. J. Geol. Soc. London. 158, 831–841. https://doi.org/10.1144/jgs.158.5.831Fairchild, I.J., Treble, P.C., 2009. Trace elements in speleothems as recorders of environmental change. Quat. Sci. Rev. 28, 449–468. https://doi.org/10.1016/j.quascirev.2008.11.007Farquhar, G.D., 1983. On the Nature of Carbon Isotope Discrimination in C4 Species. Aust. J. Plant Physiol. 10, 205–226.Farquhar, G.D., Ehleringer, J.R., Hubick, K.T., 1989. Carbon Isotope Discrimination and Photosynthesis. Annu. Rev. Plant Physiol. Plant Mol. Biol. 40, 503–537.Finné, M., Holmgren, K., Shen, C.C., Hu, H.M., Boyd, M., Stocker, S., 2017. Late Bronze Age climate change and the destruction of the Mycenaean palace of Nestor at Pylos. PLoS One 12, e0189447. https://doi.org/10.1371/journal.pone.0189447Fleitmann, D., Cheng, H., Badertscher, S., Edwards, R.L., Mudelsee, M., Göktürk, O.M., Fankhauser, A., Pickering, R., Raible, C.C., Matter, A., Kramers, J., Tüysüz, O., 2009. Timing and climatic impact of Greenland inter-

stadials recorded in stalagmites from northern Turkey. Geophys. Res. Lett. 36, 1–5. https://doi.org/10.1029/2009GL040050Flohr, P., Fleitmann, D., Zorita, E., Sadekov, A., Cheng, H., Bosomworth, M., Edwards, L., Matthews, W., Matthews, R., 2017. Late Holocene droughts in the Fertile Crescent recorded in a speleothem from northern Iraq. Geophys. Res. Lett. 44, 1528–1536. https://doi.org/10.1002/2016GL071786Fohlmeister, J., Voarintsoa, N.R.G., Lechleitner, F.A., Boyd, M., Brandtstätter, S., Jacobson, M.J., Oster, J.L., 2020. Main controls on the stable carbon isotope composition of speleothems. Geochim. Cosmochim. Acta 279, 67–87. https://doi.org/10.1016/j.gca.2020.03.042Forti, P., Postpischl, D., 1984. Seismotectonic and paleoseismic analyses using karst sediments. Mar. Geol. 55, 145–161. https://doi.org/10.1016/0025-3227(84)90138-5Fuller, B.T., De Cupere, B., Marinova, E., Van Neer, W., Waelkens, M., Richards, M.P., 2012. Isotopic reconstruction of human diet and animal husbandry practices during the Classical-Hellenistic, imperial, and Byzantine periods at Sagalassos, Turkey. Am. J. Phys. Anthropol. 149, 157–171. https://doi.org/10.1002/ajpa.22100Gates, M.-H., 1997. Archaeology in Turkey. Am. J. Archaeol. 101, 241. https://doi.org/10.2307/506511Genty, D., Baker, A., Massault, M., Proctor, C., Gilmour, M., Pons-Branchu, E., Hamelin, B., 2001. Dead carbon in stalagmites: Carbonate bedrock paleodissolution vs. ageing of soil organic matter. Implications for 13C variations in speleotherms. Geochim. Cosmochim. Acta 65, 3443–3457. https://doi.org/10.1016/S0016-7037(01)00697-4Gilli, É., 2005. Point sur l'utilisation des spéléothèmes comme indicateurs de paléosismicité ou de néotectonique. Comptes Rendus - Geosci. 337, 1208–1215. https://doi.org/10.1016/j.crte.2005.05.008Gilli, É., 2004. Glacial causes of damage and difficulties to use speleothems as palaeoseismic indicators. Geodin. Acta 17, 229–240. https://doi.org/10.3166/ga.17.229-240Giorgi, F., 2006. Climate change hot-spots. Geophys. Res. Lett. 33, 1–4. https://doi.org/10.1029/2006GL025734Göktürk, O.M., 2011. Climate in the Eastern Mediterranean through the Holocene inferred from Turkish stalagmites (PhD Thesis). University of Bern, Switzerland.Göktürk, O.M., Fleitmann, D., Badertscher, S., Cheng, H., Edwards, R.L., Leuenberger, M., Fankhauser, A., Tüysüz, O., Kramers, J., 2011. Climate on the southern Black Sea coast during the Holocene: Implications from the Sofular Cave record. Quat. Sci. Rev. 30, 2433–2445. https://doi.org/10.1016/j.quascirev.2011.05.007Heinrich, I., Touchan, R., Dorado Liñán, I., Vos, H., Helle, G., 2013. Winter-to-spring temperature dynamics in Turkey derived from tree rings since AD 1125. Clim. Dyn. 41, 1685–1701. https://doi.org/10.1007/s00382-013-1702-3Helama, S., Jones, P.D., Briffa, K.R., 2017. Dark Ages Cold Period: A literature review and directions for future research. Holocene. https://doi.org/10.1177/0959683617693898Henderson, S.A., von Caemmerer, S., Farquhar, G.D., 1992. Short-term Measurements of Carbon Isotope Discrimination in Several C4 Species. Aust. J. Plant Physiol. 19, 263–285.Hendy, C.H., 1971. The isotopic geochemistry of speleothems-I. The calculation of the effects of different modes of formation on the isotopic composition of speleothems and their applicability as palaeoclimatic indicators. Geochim. Cosmochim. Acta 35,

801–824. https://doi.org/10.1016/0016-7037(71)90127-XHörandner, W., Carr, A.W., 2005. Chi Rho, in: Kazhdan, A.P. (Ed.), The Oxford Dictionary of Byzantium. Oxford University Press, Oxford.IAEA/WMO, 2021. Global Network of Isotopes in Precipitation [WWW Document]. URL http://www.iaea.org/water (accessed 7.17.20).Izdebski, A., 2012. A rural world in transition: Asia Minor from Late Antiquity into the early Middle Ages. Taubenschlag Foundation, Berlin.Johnson, K.R., Hu, C., Belshaw, N.S., Henderson, G.M., 2006. Seasonal trace-element and stable-isotope variations in a Chinese speleothem: The potential for high-resolution paleomonsoon reconstruction. Earth Planet. Sci. Lett. 244, 394–407. https://doi.org/10.1016/j.epsl.2006.01.064Jones, M.D., Abu-Jaber, N., AlShdaifat, A., Baird, D., Cook, B.I., Cuthbert, M.O., Dean, J.R., Djamali, M., Eastwood, W., Fleitmann, D., Haywood, A., Kwiecien, O., Larsen, J., Maher, L.A., Metcalfe, S.E., Parker, A., Petrie, C.A., Primmer, N., Richter, T., Roberts, N., Roe, J., Tindall, J.C., Ünal-İmer, E., Weeks, L., 2019. 20,000 years of societal vulnerability and adaptation to climate change in southwest Asia. Wiley Interdiscip. Rev. Water 6, e1330. https://doi.org/10.1002/wat2.1330Jones, M.D., Roberts, C.N., Leng, M.J., Türkeş, M., 2006. A high-resolution late Holocene lake isotope record from Turkey and links to North Atlantic and monsoon climate. Geology 34, 361–364. https://doi.org/10.1130/G22407.1Kaniewski, D., Marriner, N., Cheddadi, R., Morhange, C., Bretschneider, J., Jans, G., Otto, T., Luce, F., Van Campo, E., 2019. Cold and dry outbreaks in the eastern Mediterranean 3200 years ago. Geology 47, 933–937. https://doi.org/10.1130/g46491.1Kaniewski, D., Paulissen, E., De Laet, V., Dossche, K., Waelkens, M., 2007. A high-resolution Late Holocene landscape ecological history inferred from an intramontane basin in the Western Taurus Mountains, Turkey. Quat. Sci. Rev. 26, 2201–2218. https://doi.org/10.1016/j.quascirev.2007.04.015Kaniewski, D., Van Campo, E., Guiot, J., Le Burel, S., Otto, T., Baeteman, C., 2013. Environmental Roots of the Late Bronze Age Crisis. PLoS One 8, 1–10. https://doi.org/10.1371/journal.pone.0071004Kaptijn, E., Poblome, J., Vanhaverbeke, H., Bakker, J., Waelkens, M., 2013. Societal changes in the Hellenistic, Roman and early Byzantine periods. Results from the Sagalassos Territorial Archaeological Survey 2008 (southwest Turkey). Anatol. Stud. 63, 75–95. https://doi.org/10.1017/S0066154613000057Karaca, M., Deniz, A., Tayanç, M., 2000. Cyclone track variability over Turkey in association with regional climate. Int. J. Climatol. 20, 1225–1236. https://doi.org/10.1002/1097-0088(200008)20:10<1225::AID-JOC535>3.0.CO;2-1Knapp, A.B., Manning, S.W., 2016. Crisis in Context: The End of the Late Bronze Age in the Eastern Mediterranean. Am. J. Archaeol. 120, 99–149. https://doi.org/10.3764/aja.120.1.0099Kokkinia, C., 2000. Die Opramoas-Inschrift von Rhodiapolis: Euergetismus und Soziale Elite in Lykien. Rudolf Habelt, Bonn.Kutiel, H., Benaroch, Y., 2002. North Sea-Caspian pattern (NCP) - An upper level atmospheric teleconnection affecting the Eastern Mediterranean: Identification and definition. Theor. Appl. Climatol. 71, 17–28. https://doi.org/10.1007/s704-002-8205-xKutiel, H., Maheras, P., Türkeş, M., Paz, S., 2002. North Sea - Caspian Pattern (NCP) - An upper level atmo-

spheric teleconnection affecting the eastern Mediterranean - Implications on the regional climate. Theor. Appl. Climatol. https://doi.org/10.1007/s00704-002-0674-8Kutiel, H., Türkeş, M., 2005. New evidence for the role of the North Sea - Caspian Pattern on the temperature and precipitation regimes in continental Central Turkey. Geogr. Ann. Ser. A Phys. Geogr. 87, 501–513. https://doi.org/10.1111/j.0435-3676.2005.00274.xKuzucuoğlu, C., Dörfler, W., Kunesch, S., Goupille, F., 2011. Mid- to late-Holocene climate change in central Turkey: The tecer lake record. Holocene 21, 173–188. https://doi.org/10.1177/0959683610384163Lewis, S.C., Gagan, M.K., Ayliffe, L.K., Zhao, J. xin, Hantoro, W.S., Treble, P.C., Hellstrom, J.C., LeGrande, A.N., Kelley, M., Schmidt, G.A., Suwargadi, B.W., 2011. High-resolution stalagmite reconstructions of Australian-Indonesian monsoon rainfall variability during Heinrich stadial 3 and Greenland interstadial 4. Earth Planet. Sci. Lett. 303, 133–142. https://doi.org/10.1016/j.epsl.2010.12.048Lionello, P., 2012. The Climate of the Mediterranean Region: From the Past to the Future. Elsevier Inc., London.Luterbacher, J., Garcia-Herrera, R., Akçer-Ön, S., Allan, R., Alvarez-Castro, M.C., Benito, G., Booth, J., Buntgen, U., Cagatay, N., Colombaroli, D., Davis, B., Esper, J., Felis, T., Fleitmann, D., Frank, D., Gallego, D., Garcia-Bustamante, E., Glaser, R., González-Rouco, J.F., Goosse, H., Kiefer, T., Macklin, M.G., Manning, S., Montagna, P., Newman, L., Power, M.J., Rath, V., Ribera, P., Riemann, D., Roberts, N., Sicre, M.A., Silenzi, S., Tinner, W., Valero-Garces, B., van der Schrier, G., Tzedakis, C., Vanniere, B., Vogt, S., Wanner, H., Werner, J.P., Willet, G., Williams, M.H., Xoplaki, E., Zerefos, C., Zorita, E., 2012. A review of 2000 years of paleoclimatic evidence in the Mediterranean, in: Lionello, P. (Ed.), The Climate of the Mediterranean Region: From the Past to the Future. Elsevier, Amsterdam, pp. 87–185.Malalas, J., 2017. The Chronicle of John Malalas, The Chronicle of John Malalas. Australian Association for Byzantine Studies, Melbourne. https://doi.org/10.1163/9789004344600Manning, S.W., Lorentzen, B., Welton, L., Batiuk, S., Harrison, T.P., 2020. Beyond megadrought and collapse in the Northern Levant: The chronology of Tell Tayinat and two historical inflection episodes, around 4.2ka BP, and following 3.2ka BP, PLoS ONE. https://doi.org/10.1371/journal.pone.0240799Mannocchi, F., Todisco, F., Vergni, L., 2004. Agricultural drought: indices, definition and analysis, in: The Basis of Civilization-Water Science? (Proceedings of the UNESCO/IAIIS/IWIIA Symposium Held in Rome. December 2003). IAHS Publ, Rome.Masson-Delmotte, V., Schulz, M., Abe-Ouchi, A., Beer, J., Ganopolski, A., Gonzalez-Rouco, J.F., Jansen, E., Lambeck, K., Luterbacher, J., Naish, T., Osborn, T., Otto-Bliesner, B., Quinn, T., Ramesh, R., Rojas, M., Shao, X., Timmerman, A., 2013. Information from Paleoclimate Archives, in: Stocker, T.F., Qin, D., Plattner, G.-K., Tignor, M., Allen, S.K., Boschung, J., Nauels, A., Xia, Y., Bex, V., Midgley, P.M. (Eds.), Climate Change 2013: The Physical Science Basis. Contribution of Working Group I to the Fifth Assessment Report of the Intergovernmental Panel on Climate Change. Cambridge University Press, Cambridge, pp. 383–464.Mayewski, P.A., Rohling, E.E., Stager, J.C., Karlén, W., Maasch, K.A., Meeker, L.D., Meyerson, E.A., Gasse, F., van

Kreveld, S., Holmgren, K., Lee-Thorp, J., Rosqvist, G., Rack, F., Staubwasser, M., Schneider, R.R., Steig, E.J., 2004. Holocene climate variability. Quat. Res. 62, 243–255. https://doi.org/10.1016/j.yqres.2004.07.001McDermott, F., Schwarcz, H.P., Rowe, P.J., 2006. Isotopes in speleothems, in: Leng, M.J. (Ed.), Isotopes in Palaeoenvironmental Research. Springer, Dordrecht, The Netherlands, pp. 185–226.McDonald, J., Drysdale, R., Hill, D., 2004. The 2002-2003 El Niño recorded in Australian cave drip waters: Implications for reconstructing rainfall histories using stalagmites. Geophys. Res. Lett. 31, 1–4. https://doi.org/10.1029/2004GL020859Morin, E., Ryb, T., Gavrieli, I., Enzel, Y., 2019. Mean, variance, and trends of Levant precipitation over the past 4500 years from reconstructed Dead Sea levels and stochastic modeling. Quat. Res. (United States) 91, 751–767. https://doi.org/10.1017/qua.2018.98Newfield, T.P., 2018. The Climate Downturn of 536-50, in: White, S., Pfister, C., Mauelshagen, F. (Eds.), The Palgrave Handbook of Climate History. Palgrave Macmillan, London, pp. 447–493. https://doi.org/10.1057/978-1-137-43020-5Öztürk, M.Z., Çetınkaya, G., Aydin, S., 2017. Köppen-Geiger İklim Sınıflandırmasına Göre Türkiye'nin İklim Tipleri - (Climate Types of Turkey According to Köppen-Geiger Climate Classification). Istanbul Univ. J. Geogr. 35, 17–27. https://doi.org/10.26650/jgeog330955Papadopoulos, G.A., Daskalaki, E., Fokaefs, A., Giraleas, N., 2007. Tsunami hazards in the Eastern Mediterranean: Strong earthquakes and tsunamis in the East Hellenic Arc and Trench system. Nat. Hazards Earth Syst. Sci. 7, 57–64. https://doi.org/10.5194/nhess-7-57-2007Park, Jungjae, Park, Jinheum, Yi, S., Cheul Kim, J., Lee, E., Choi, J., 2019. Abrupt Holocene climate shifts in coastal East Asia, including the 8.2 ka, 4.2 ka, and 2.8 ka BP events, and societal responses on the Korean peninsula. Sci. Rep. 9, 1–16. https://doi.org/10.1038/s41598-019-47264-8Peel, M.C., Finlayson, B.L., McMahon, T.A., 2007. Updated world map of the Köppen-Geiger climate classification. Hydrol. Earth Syst. Sci. https://doi.org/10.5194/hess-11-1633-2007Peterson, T.C., Vose, R.S., 1997. An Overview of the Global Historical Climatology Network Temperature Database. Bull. Am. Meteorol. Soc. 78, 2837–2849. https://doi.org/10.1175/1520-0477(1997)078<2837:AOOTGH>2.0.CO;2Pirazzoli, P.A., Laborel, J., Stiros, S.C., 1996. Earthquake clustering in the eastern Mediterranean during historical times. J. Geophys. Res. Solid Earth 101, 6083–6097. https://doi.org/10.1029/95jb00914Poblome, J., 2015. The Economy of the Roman World as a Complex Adaptive System: Testing the Case in Second to Fifth Century CE Sagalassos, in: Erdkamp, P., Verboven, K. (Eds.), Structure and Performance in the Roman Economy: Models, Methods, and Case Studies. Éditions Latomus, Brussels, pp. 97–140.Pote, D.H., Daniel, T.C., Nichols, D.J., Moore, P.A., Miller, D.M., Edwards, D.R., 1999. Seasonal and Soil-Drying Effects on Runoff Phosphorus Relationships to Soil Phosphorus. Soil Sci. Soc. Am. J. 63, 1006–1012. https://doi.org/10.2136/sssaj1999.6341006xPsomiadis, D., Dotsika, E., Albanakis, K., Ghaleb, B., Hillaire-Marcel, C., 2018. Speleothem record of climatic changes in the northern Aegean region (Greece) from the Bronze Age to the collapse of the Roman Empire. Palaeogeogr. Palaeoclimatol. Palaeoecol. 489,

272–283. https://doi.org/10.1016/j.palaeo.2017.10.021Sariş, F., Hannah, D.M., Eastwood, W.J., 2010. Spatial variability of precipitation regimes over Turkey. Hydrol. Sci. J. 55, 234–249. https://doi.org/10.1080/02626660903546142Scholz, D., Hoffmann, D.L., 2011. StalAge - An algorithm designed for construction of speleothem age models. Quat. Geochronol. 6, 369–382. https://doi.org/10.1016/j.quageo.2011.02.002Seguin, J., Avramidis, P., Dörfler, W., Emmanouilidis, A., Unkel, I., 2020. A 2600-year high-resolution climate record from Lake Trichonida (SW Greece). E&G Quat. Sci. J. 69, 139–160. https://doi.org/10.5194/egqsj-69-139-2020Sezen, C., Partal, T., 2019. The impacts of Arctic oscillation and the North Sea Caspian pattern on the temperature and precipitation regime in Turkey. Meteorol. Atmos. Phys. 131, 1677–1696. https://doi.org/10.1007/s00703-019-00665-wSharifi, A., Pourmand, A., Canuel, E.A., Ferer-Tyler, E., Peterson, L.C., Aichner, B., Feakins, S.J., Daryaee, T., Djamali, M., Beni, A.N., Lahijani, H.A.K., Swart, P.K., 2015. Abrupt climate variability since the last deglaciation based on a high-resolution, multi-proxy peat record from NW Iran: The hand that rocked the Cradle of Civilization? Quat. Sci. Rev. 123, 215–230. https://doi.org/10.1016/j.quascirev.2015.07.006Similox-Tohon, D., Sintubin, M., Muchez, P., Verhaert, G., Vanneste, K., Fernandez, M., Vandycke, S., Vanhaverbeke, H., Waelkens, M., 2006. The identification of an active fault by a multidisciplinary study at the archaeological site of Sagalassos (SW Turkey). Tectonophysics 420, 371–387. https://doi.org/10.1016/j.tecto.2006.03.026Sinha, A., Kathayat, G., Weiss, H., Li, H., Cheng, H., Reuter, J., Schneider, A.W., Berkelhammer, M., Adalı, S.F., Stott, L.D., Lawrence Edwards, R., 2019. Role of climate in the rise and fall of the Neo-Assyrian Empire. Sci. Adv 5, 6656–6669.Steinhilber, F., Beer, J., Fro, C., 2009. Total solar irradiance during the Holocene 36, 1–5. https://doi.org/10.1029/2009GL040142Stiros, S.C., 2001. The AD 365 Cret earthquake and possible seismic clustering during the fourth to sixth centuries AD in the Eastern Mediterranean: A review of historical and archaeological data. J. Struct. Geol. 23, 545–562. https://doi.org/10.1016/S0191-8141(00)00118-8Talloen, P., 2015. Cult in Pisidia. Religious Practice in Southwestern Asia Minor from Alexander the Great to the Rise of Christianity. (Studies in Eastern Mediterranean Archaeology, 10). Brepols, Turnhout.Tan, O., Tapirdamaz, M.C., Yörük, A., 2008. The earthquake catalogues for Turkey. Turkish J. Earth Sci. 17, 405–418.Tanner, S.D., Baranov, V.I., Bandura, D.R., 2002. Reaction cells and collision cells for ICP-MS: A tutorial review. Spectrochim. Acta - Part B At. Spectrosc. 57, 1361–1452. https://doi.org/10.1016/S0584-8547(02)00069-1Treble, P., Shelley, J.M.G., Chappell, J., 2003. Comparison of high resolution sub-annual records of trace elements in a modern (1911-1992) speleothem with instrumental climate data from southwest Australia. Earth Planet. Sci. Lett. 216, 141–153. https://doi.org/10.1016/S0012-821X(03)00504-1Tremaine, D.M., Froelich, P.N., 2013. Speleothem trace element signatures: A hydrologic geochemical study of modern cave dripwaters and farmed calcite. Geochim. Cosmochim. Acta 121, 522–545. https://doi.org/10.1016/j.gca.2013.07.026Tudryn, A., Tucholka, P., Özgûr, N., Gibert, E., Elitok, O., Kamaci, Z., Massault,

M., Poisson, A., Platevoet, B., 2013. A 2300-year record of environmental change from SW Anatolia, Lake Burdur, Turkey. J. Paleolimnol. 49, 647–662. https://doi.org/10.1007/s10933-013-9682-1Türkeş, M., Erlat, E., 2009. Winter mean temperature variability in Turkey associated with the North Atlantic Oscillation. Meteorol. Atmos. Phys. 105, 211–225. https://doi.org/10.1007/s00703-009-0046-3Türkeş, M., Erlat, E., 2003. Precipitation changes and variability in Turkey linked to the North Atlantic oscillation during the period 1930-2000. Int. J. Climatol. 23, 1771–1796. https://doi.org/10.1002/joc.962Ulbrich, U., Lionello, P., Belušić, D., Jacobeit, J., Knippertz, P., Kuglitsch, G., Leckebusch, G.C., Luterbacher, J., Maugeri, M., Maheras, P., Nissen, K.M., Pavan, V., Pinto, J.G., Saaroni, H., Seubert, S., Toreti, A., Xoplaki, E., Ziv, B., 2012. Climate of the Mediterranean: Synoptic Patterns, Temperature, Precipitation, Winds and their Extremes, in: Lionello, P. (Ed.), The Climate of the Mediterranean Region: From the Past to the Future. Elsevier, Amsterdam, pp. 301–346.Ülgen, U.B., Franz, S.O., Biltekin, D., Çagatay, M.N., Roeser, P.A., Doner, L., Thein, J., 2012. Climatic and environmental evolution of Lake Iznik (NW Turkey) over the last 4700 years. Quat. Int. 274, 88–101. https://doi.org/10.1016/j.quaint.2012.06.016Unal, Y.S., Deniz, A., Toros, H., Incecik, S., 2012. Temporal and spatial patterns of precipitation variability for annual, wet, and dry seasons in Turkey. Int. J. Climatol. 32, 392–405. https://doi.org/10.1002/joc.2274University of East Anglia Climatic Research Unit, Harris, I.C., Jones, P.D., Osborn, T., 2020. CRU TS4.04: Climatic Research Unit (CRU) Time-Series (TS) version 4.04 of high-resolution gridded data of month-by-month variation in climate (Jan. 1901- Dec. 2019). Norwich.Van Geel, B., Coope, G.R., Van Der Hammen, T., 1989. Palaeoecology and stratigraphy of the lateglacial type section at Usselo (the Netherlands). Rev. Palaeobot. Palynol. 60. https://doi.org/10.1016/0034-6667(89)90072-9Vandam, R., Kaptijn, E., Broothaerts, N., De Cupere, B., Marinova, E., Van Loo, M., Verstraeten, G., Poblome, J., 2019. "Marginal" Landscapes: Human Activity, Vulnerability, and Resilience in the Western Taurus Mountains (Southwest Turkey). J. East. Mediterr. Archaeol. Herit. Stud. 7, 432–450. https://doi.org/doi: 10.5325/jeasmedarcher-stu.7.4.0432Vermoere, M., Bottema, S., Vanhecke, L., Waelkens, M., Paulissen, E., Smets, E., 2002. Palynological evidence for late-Holocene human occupation recorded in two wetlands in SW Turkey. The Holocene 12, 569–584. https://doi.org/10.1191/0959683602hl568rpVicente-Serrano, S.M., Beguería, S., López-Moreno, J.I., 2010. A multiscalar drought index sensitive to global warming: The standardized precipitation evapotranspiration index. J. Clim. 23, 1696–1718. https://doi.org/10.1175/2009JCLI2909.1Waelkens, M., Sintubin, M., Muchez, P., Paulissen, E., 2000. Archaeological, geomorphological and geological evidence for a major earthquake at Sagalassos (SW Turkey) around the middle of the seventh century AD. Geol. Soc. Spec. Publ. 171, 373–383. https://doi.org/10.1144/GSL.SP.2000.171.01.27Wanner, H., Wanner, H., Mercolli, L., Mercolli, L., Grosjean, M., Grosjean, M., Ritz, S.P., 2015. Holocene climate variability and change; a data-based review. J. Geol. Soc. London. 172, 254–263. https://doi.org/10.1144/jgs2013-101Wassenburg, J.A., Riechelmann,

S., Schröder-Ritzrau, A., Riechelmann, D.F.C., Richter, D.K., Immenhauser, A., Terente, M., Constantin, S., Hachenberg, A., Hansen, M., Scholz, D., 2020. Calcite Mg and Sr partition coefficients in cave environments: Implications for interpreting prior calcite precipitation in speleothems. Geochim. Cosmochim. Acta 269, 581–596. https://doi.org/10.1016/j.gca.2019.11.011Woodbridge, J., Roberts, C.N., Palmisano, A., Bevan, A., Shennan, S., Fyfe, R., Eastwood, W.J., Izdebski, A., Çakırlar, C., Woldring, H., Broothaerts, N., Kaniewski, D., Finné, M., Labuhn, I., 2019. Pollen-inferred regional vegetation patterns and demographic change in Southern Anatolia through the Holocene. Holocene. https://doi.org/10.1177/0959683619826635Xoplaki, E., Luterbacher, J., Wagner, S., Zorita, E., Fleitmann, D., Preiser-Kapeller, J., Sargent, A.M., White, S., Toreti, A., Haldon, J.F., Mordechai, L., Bozkurt, D., Akçer-Ön, S., Izdebski, A., 2018. Modelling Climate and Societal Resilience in the Eastern Mediterranean in the Last Millennium. Hum. Ecol. 46, 363–379. https://doi.org/10.1007/s10745-018-9995-9